Electronic supplementary materials *Mendeleev Commun.*, 2024, **34**, 119–121

Myrtenyl-bispidine containing azole: synthesis and antifungal activity

Nikolai S. Li-Zhulanov, Konstantin Yu. Ponomarev, Suat Sari, Dolunay Gülmez, Sevtap Arikan-Akdagli, Vyacheslav I. Krasnov, Evgenii V. Suslov, Konstantin P. Volcho and Nariman F. Salakhutdinov

Table of content

1. Experimental……S2
2. NMR spectra……S5
3. HRMS……S14
4. Antifungal activity……S15
5. Molecular docking……S15

Experimental

(1*R*)-(−)-Myrtenol >97% (*ee* 95%), (Sigma-Aldrich (St. Louis, MO, USA)), and other reagents and solvents were purchased from commercial suppliers (Sigma-Aldrich (St. Louis, MO, USA), Acros (Waltham, MA, USA)) and used as received. Column chromatography (CC) was performed on silica gel (SiO_2; 60–200 μ; Macherey-Nagel (Dueren, Germany)) using hexane/EtOAc 100:0 → 0:100 as mobile phase. GC-MS was performed using Agilent 7890A gas chromatograph (Santa Clara, CA, USA) equipped with a quadrupole mass spectrometer Agilent 5975C as detector; quartz column HP-5MS (copolymer 5% diphenyl and 95% dimethylsiloxane) of length 30 m, internal diameter 0.25 mm, and stationary phase film thickness 0.25 μm. ^{1}H and ^{13}C NMR spectra were recorded using Bruker Avance-III 600 apparatus (Billerica, MA, USA) at 600.30 MHz (^{1}H) and 150.95 MHz (^{13}C) and Bruker Avance 400 (Bruker Corporation, Karlsruhe, Germany) apparatus 400.13 MHz (^{1}H), 100.61 MHz (^{13}C) and 376.45 MHz (^{19}F) J in Hz. Structure determinations were made by analyzing the ^{1}H NMR spectra, including ^{1}H–^{1}H 2D homonuclear correlation, J-modulated ^{13}C NMR spectra (JMOD), and ^{13}C–^{1}H 2D heteronuclear correlation with one-bond and long-range spin-spin coupling constants (C-H COSY, $^{1}J(C,H)$ = 135 Hz; HSQC, $^{1}J(C,H)$ = 145 Hz; HMBC, $^{2,3}J(C,H)$ = 7 Hz). HR-MS was performed using Bruker Daltonics GmbH micrOTOF-Q spectrometer (Bremen, Germany) applying electrospray ionization at positive ion mode. Agilent 6890N gas chromatograph (Santa Clara, CA, USA) equipped with a quadrupole mass spectrometer Agilent 5973 N as a detector. All the target compounds reported in this paper have a purity of at least 95%. 1-((2-(2,4-Difluorophenyl)oxiran-2-yl)methyl)-1*H*-1,2,4-triazole **5** was synthesized according to work[S1]. (1*R*,5*S*)-3-(((1*R*,5*S*)-6,6-Dimethylbicyclo[3.1.1]hept-2-en-2-yl)methyl)-1,5-dimethyl-3,7-diazabicyclo[3.3.1]nonane **8** was synthesized from (−)-myrtenol according to work[S2].

1-(2,4-Difluorophenyl)-2-(1*H*-1,2,4-triazol-1-yl)ethan-1-one 4.

^{1}H NMR ($CDCl_3$, δ, ppm, J, Hz): 5.53 (s, 2H), 6.92 (ddd, 1H, J=11.0, 8.4, 2.3 Hz), 6.98 (ddd, 1H, J=9.6, 7.0, 2.3 Hz), 7.91 (s, 1H), 7.96 (td, 1H, J=8.5, 7.0 Hz), 8.15 (s, 1H). ^{13}C NMR ($CDCl_3$, δ, ppm): 58.4 (d, J=13.5 Hz, CH_2), 105.0 (t, J=26.6 Hz, CH), 113.2 (d, J=21.7 Hz, CH), 119.0 (d, J=11.4 Hz, CH), 133.1 (dd, J=10.7, 3.9 Hz, CH), 145.0 (CH), 151.9 (CH), 163.2 (dd, J=256.9, 12.7 Hz, C–F), 166.8 (dd, J=260.3, 12.6 Hz, C–F), 187.7 (C=O); HRMS: 224.0624 $[M+H]^+$; calcd. 224.0635 $(C_{10}H_8F_2N_3O)^+$.

1-{[2-(2,4-Difluorophenyl)oxiran-2-yl]methyl}-1*H*-1,2,4-triazole 5.

^{1}H NMR ($CDCl_3$, δ, ppm, J, Hz): 8.08 (s, 1H), 7.86 (s, 1H), 7.20−7.11 (m, 1H), 6.86−6.75 (m, 2H), 4.82 (d, J = 14.8 Hz, 1H), 4.49 (d, J = 14.8 Hz, 1H), 2.93 (d, J = 4.6 Hz, 1H), 2.87 (d, J = 4.6 Hz, 1H). ^{13}C NMR ($CDCl_3$, δ, ppm): 164.4, 164.3, 161.9, 161.8, 161.7, 159.4, 159.2, 151.8, 144.1, 129.64, 129.59, 129.55, 129.49, 111.90, 111.87, 111.69, 111.65, 104.3, 104.1, 103.8, 56.3, 53.59, 53.55, 52.2. LRMS: 238.1 $[M + H]^+$; calcd. 237.1 $(C_{11}H_9F_2N_3O)^+$.

(1*R*,5*S*)-2-Bromomethyl-6,6-dimethylbicyclo[3.1.1]hept-2-ene 7.

^{1}H NMR ($CDCl_3$, δ, ppm, J, Hz): 2.10-2.46 (5H, m, H-1, 4, 5, 7b), 5.68 (1H, s, H-3), 1.18 (1H, d, J=8.5, H-7a), 0.84 (3H, s, Me-8), 1.32 (3H, s, Me-9), 3.95 (2H, s, H-10). ^{13}C NMR ($CDCl_3$, δ, ppm): 44.9 (C-1), 144.2 (C-2), 123.1 (C-3), 31.3 (C-4), 40.4 (C-5), 38.0 (C-6), 31.6 (C-7), 21.1 (C-8), 26.0 (C-9), 37.7 (C-10).

The synthesis of compound **8** from the reaction between of **7** and **6** proceeds firstly through the formation of salt **A** (Scheme S1). Then, the reaction of **A** with alkali leads to intermediate **B**, that eliminated a formaldehyde molecule transforming into compound **8**[S3].

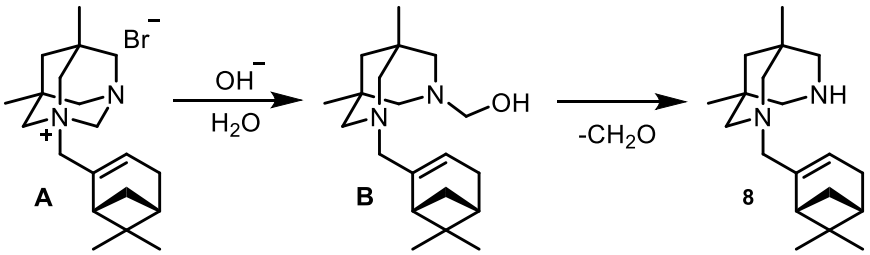

Scheme S1 Possible mechanism of formation product **8**.

Synthesis of 2-(2,4-difluorophenyl)-1-(7-{[(1*R*,5*S*)-6,6-dimethylbicyclo[3.1.1]hept-2-en-2-yl]methyl}-1,5-dimethyl-3,7-diazabicyclo[3.3.1]non-3-yl)-3-(1*H*-1,2,4-triazol-1-yl)propan-2-ol 2.

To a solution of oxirane **5** (85 mg, 0.36 mmol, 1 eq) in ethanol (10 mL) myrtenyl-bispidine **8** (123 mg, 0.43 mmol, 1.2 eq) and NEt_3 (62 µL, 0.43 mmol, 1.2 eq) were added. The reaction mixture was refluxed until the TLC analysis (1:1 hexane/EtOAc) demonstrated the total consumption of oxirane. Then, the reaction mixture was washed with brine (3 × 20 mL) and dried over anhydrous Na_2SO_4. The desiccant was filtered, the filtrate was concentrated under reduced pressure and the product was purified by column chromatography on silica gel with eluent EtOAc in hexane from 0% to 100%. The compound **2** (125 mg, 55%) was obtained as a yellow oil.

NMR spectra were recorded for a mixture (1:1) of diastereomers, the designations (H-1, H-1ds) and (C-1, C-1ds) are employed to distinguish signals from diastereomers in a mixture due to signal discrimination is challenging. Also, special designations (H-c, C-c) were used for atoms 14, 15 and 17.

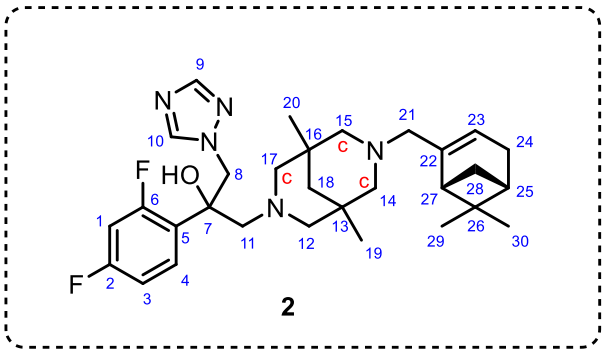

^{1}H-NMR ($CDCl_3$, δ ppm, J, Hz): 8.29 (s, 1H) and 8.27 (s, 1H) : H-10 both ds, 7.70 (s, 1H) and 7.67 (s, 1H) : H-9 both ds, 7.51-7.57 (m, 2H, H-4 both ds), 7.10 (br s, 2H, OH), 6.72-6.77 (m, 4H, H-1 both ds, H-3 both ds), 5.41 (s, 1H) and 5.39 (s, 1H) : (H-23 both ds), 4.47 (A of AB-system, J = 14.0, 1H) and 4.41 (degenerate AB-system, J ~ 14, 2H) and 4.37 (B of AB-system, J = 14.0, 1H) : (H-8 both ds), 2.95 (d, J = 12.4, 1H, H-21), 2.87 (d, J = 13.6, 2H, H-11 both ds), 2.66-2.74 (m, 4H: 2 H-21 - one ds, 2 H-c - both ds), 2.40-2.53 (m, 9H: 2 H-c - both ds, 2 H-11 - both ds, 2 H-27 - both ds, 2 H-28 - both ds, H-21), 2.29 (A of AB-system, J = 17.8, 2H, H-24 both ds), 2.20-2.26 (m, 6H: 2 H-24 both ds, 4 H-c - both ds), 2.07-2.11 (m, 2H, H-25 both ds), 1.80-1.90 (m, 4H, H-12 both ds), 1.60-1.64 (m, 2H, H-c), 1.54-1.56 (m, 2H, H-c), 1.33 (s, 3H) and 1.33 (s, 3H) : H-30 both ds, 1.17 (d, J = 8.3, 1H) and 1.15 (d, J = 7.5, 1H) : H-28 both ds, 0.91-0.95 (m, 4H, H-18 both ds), 0.85 (s, 3H) and 0.84 (s, 3H) : H-29 both ds, 0.70 (s, 3H) and 0.68 (s, 3H) : H-20 both ds, 0.51 (s, 3H) and 0.50 (s, 3H) : H-19 both ds.

^{13}C{^{1}H}-NMR ($CDCl_3$, δC): 162.27 (dd, J = 248.5, 11.9) and 162.25 (dd, J = 248.5, 11.9) : C-2 both ds, 158.89 (dd, J = 246.9, 11.8) and 158.85 (dd, J = 246.9, 11.8) : C-6 both ds, 150.31 and 150.29 (C-9 both ds), 144.82 and 144.54 (C-22 both ds), 144.57 and 144.39 (C-10 both ds), 129.35 (dd, J = 9.3, 6.4) and 129.31 (dd, J = 9.3, 6.4) : C-4 both ds, 127.93 (dd, J = 13.5, 3.9) and 127.81 (dd, J = 13.1, 3.9) : C-5 both ds, 121.65 and 121.31 (C-23 both ds), 110.84 (dd, J = 20.5, 3.3) and 110.80 (dd, J = 20.3, 3.3) : C-3 both ds, 103.96 (dd, J = 27.1, 25.5) and 103.90 (dd, J = 27.0, 25.6) : C-1 both ds, 71.96 and 71.79 (C-7 both ds), 66.19 and 66.11 (C-21 both ds), 64.99, 64.80, 64.80, 64.72, 64.54 and 64.02 (C-c both ds), 62.63 and 62.50 (C-12 both ds), 61.25 (d, J = 3.8) and 60.66 (d, J = 3.7) : C-11 both ds, 57.32 (d, J = 5.2) and 56.79 (d, J = 5.5) : C-8 both ds, 46.70 (C-18 both ds), 44.87 and 44.78 (C-27 both ds), 40.56 (C-25 both ds), 37.83 and 37.82 (C-26 both ds), 32.65, 32.60, 32.38 and 32.36 (C-13 both ds and C-16 both ds), 31.96 and 31.69 (C-28 both ds), 31.33 and 31.32 (C-24 both ds), 26.30 and 26.23 (C-30 both ds), 25.70, 25.70, 25.64, 25.51 (C-19 both ds and C-20 both ds), 21.21 and 21.00 (C-29 both ds).

^{19}F{^{1}H}-NMR ($CDCl_3$, δC): 54.38 (d, J = 7.6, 1F) and 54.23 (d, J = 7.6, 1F) : F-6 both ds, 50.99-51.03 (m, 2F, F-2 both ds). HRMS: 526.340 [M+H]+; calcd. 526.335 $(C_{30}H_{42}N_5OF_2)^+$.

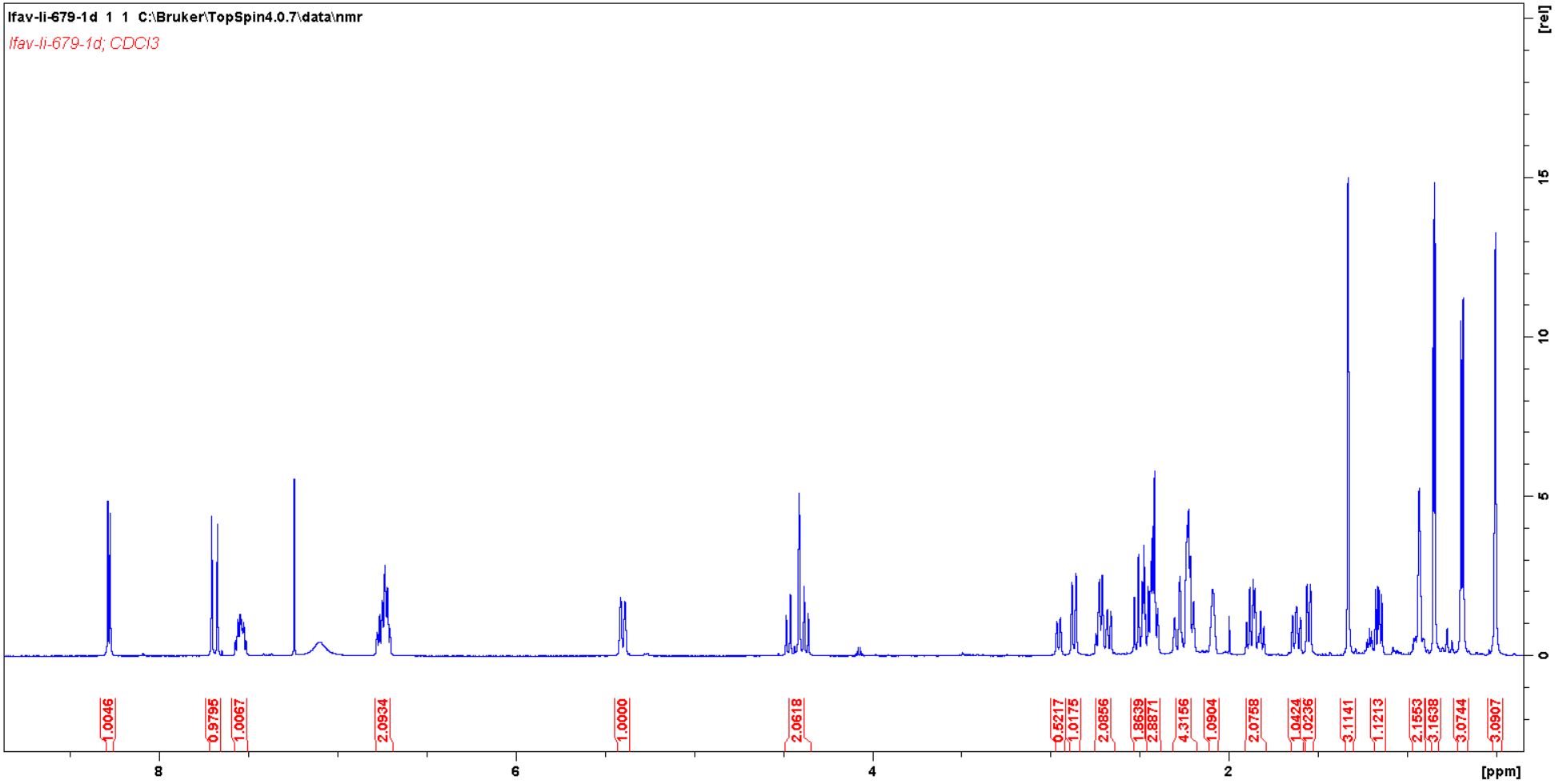

Figure S1 ^{1}H NMR spectrum of **2**.

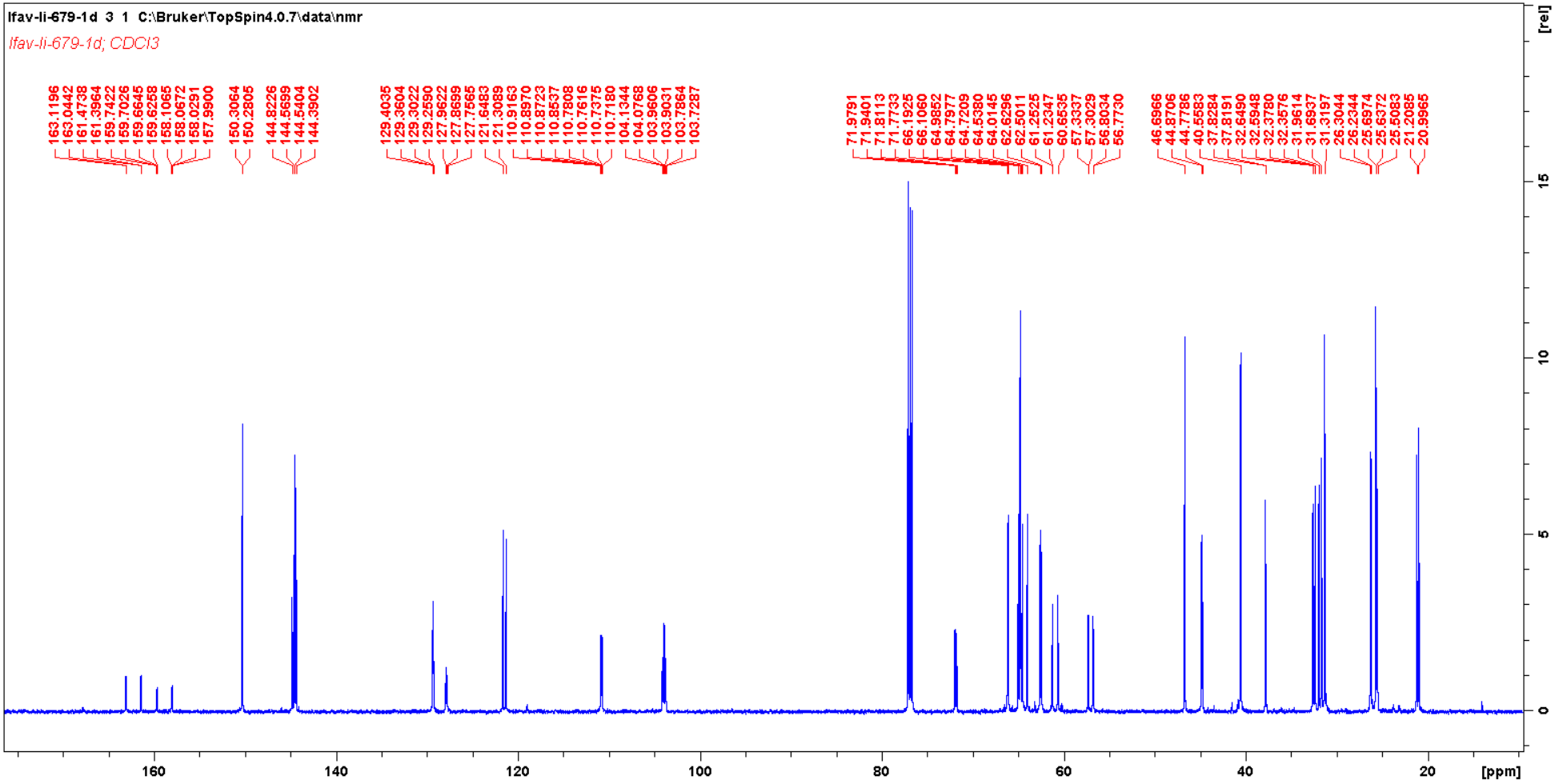

Figure S2 ^{13}C NMR spectrum of **2**.

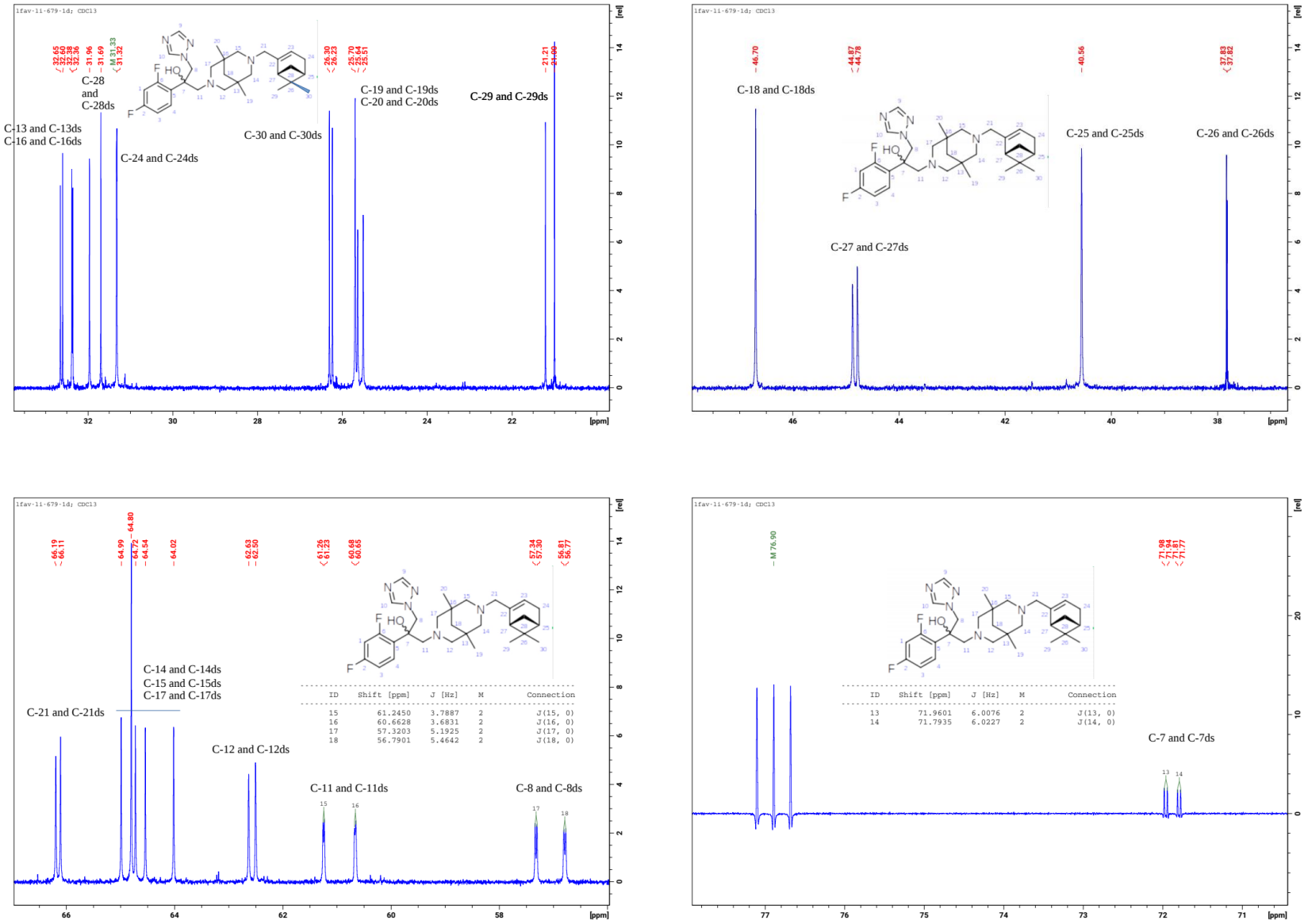

Figure S3 ^{13}C NMR spectrum of **2**.

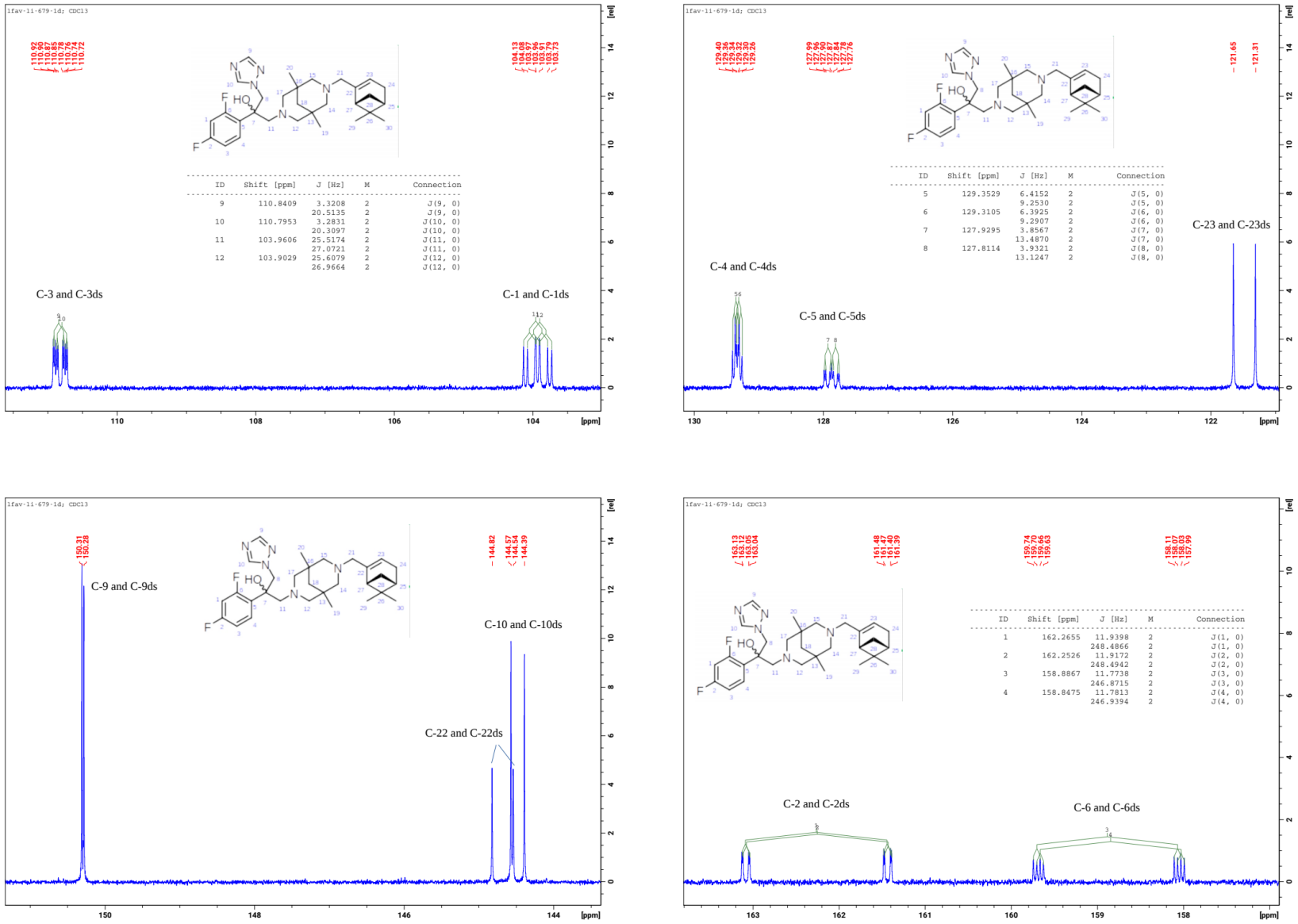

Figure S3 (continued).

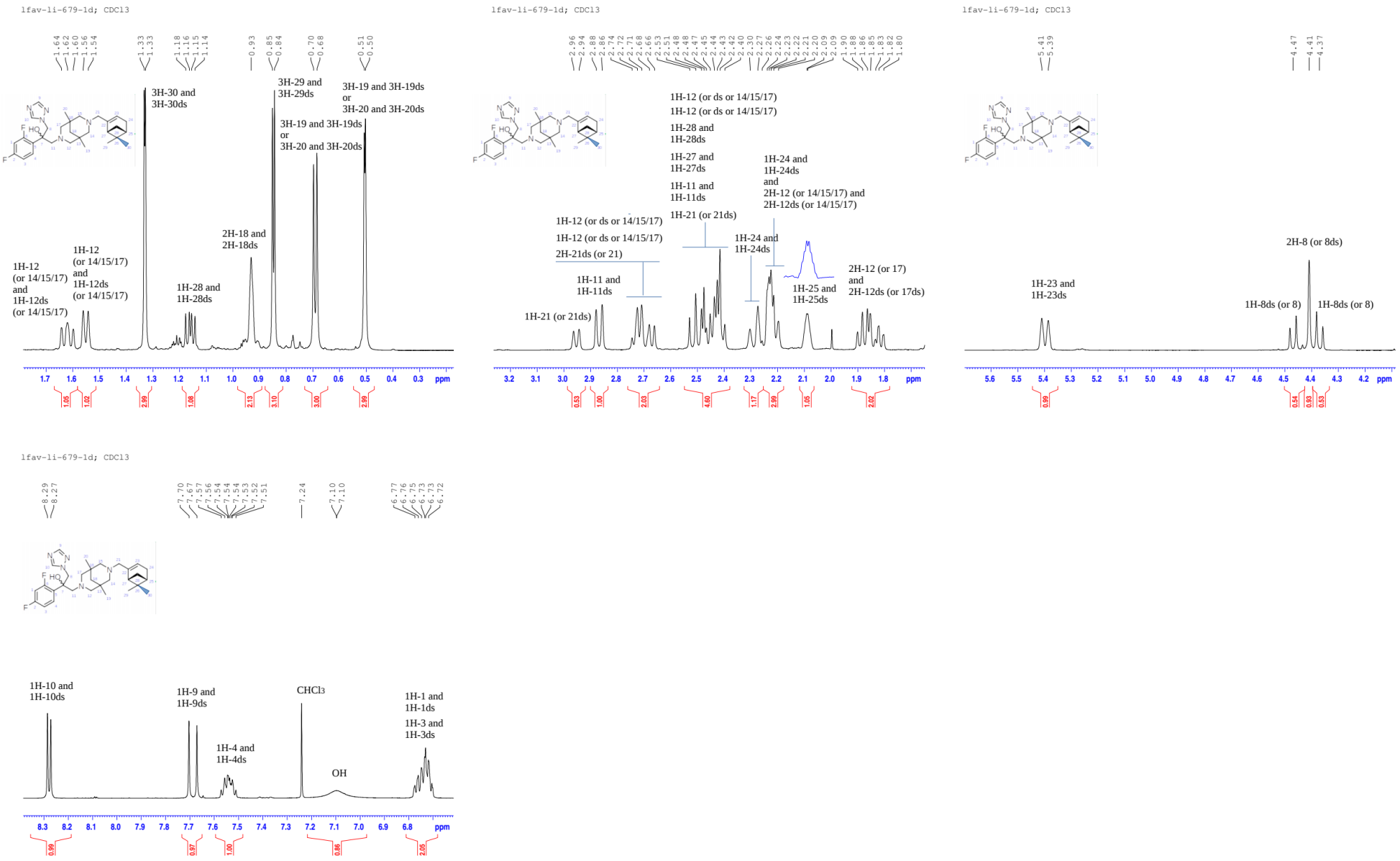

Figure S4 ^{1}H NMR spectrum of **2**.

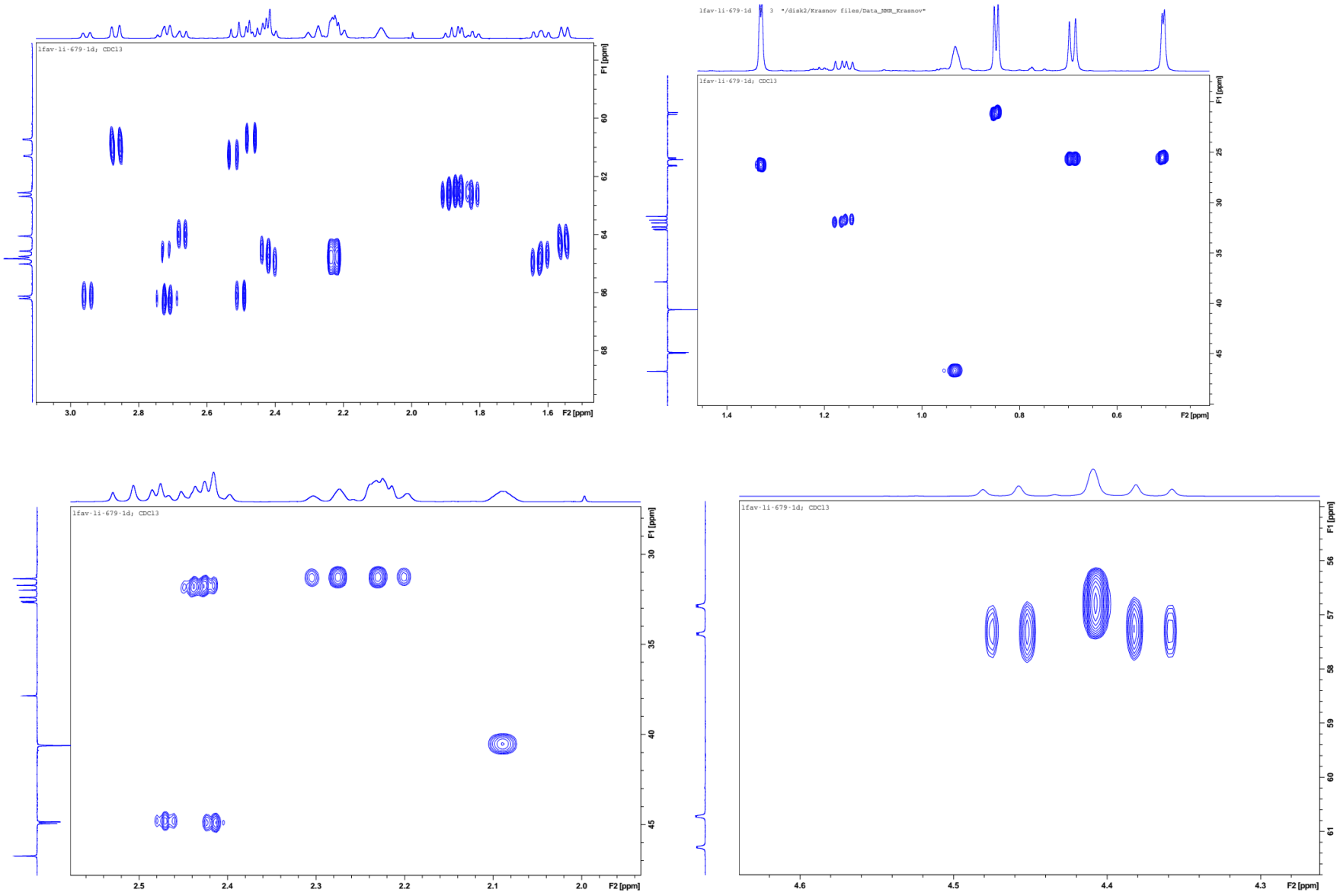

Figure S5 2D ^{1}H-^{13}C HSQC NMR spectrum of **2**.

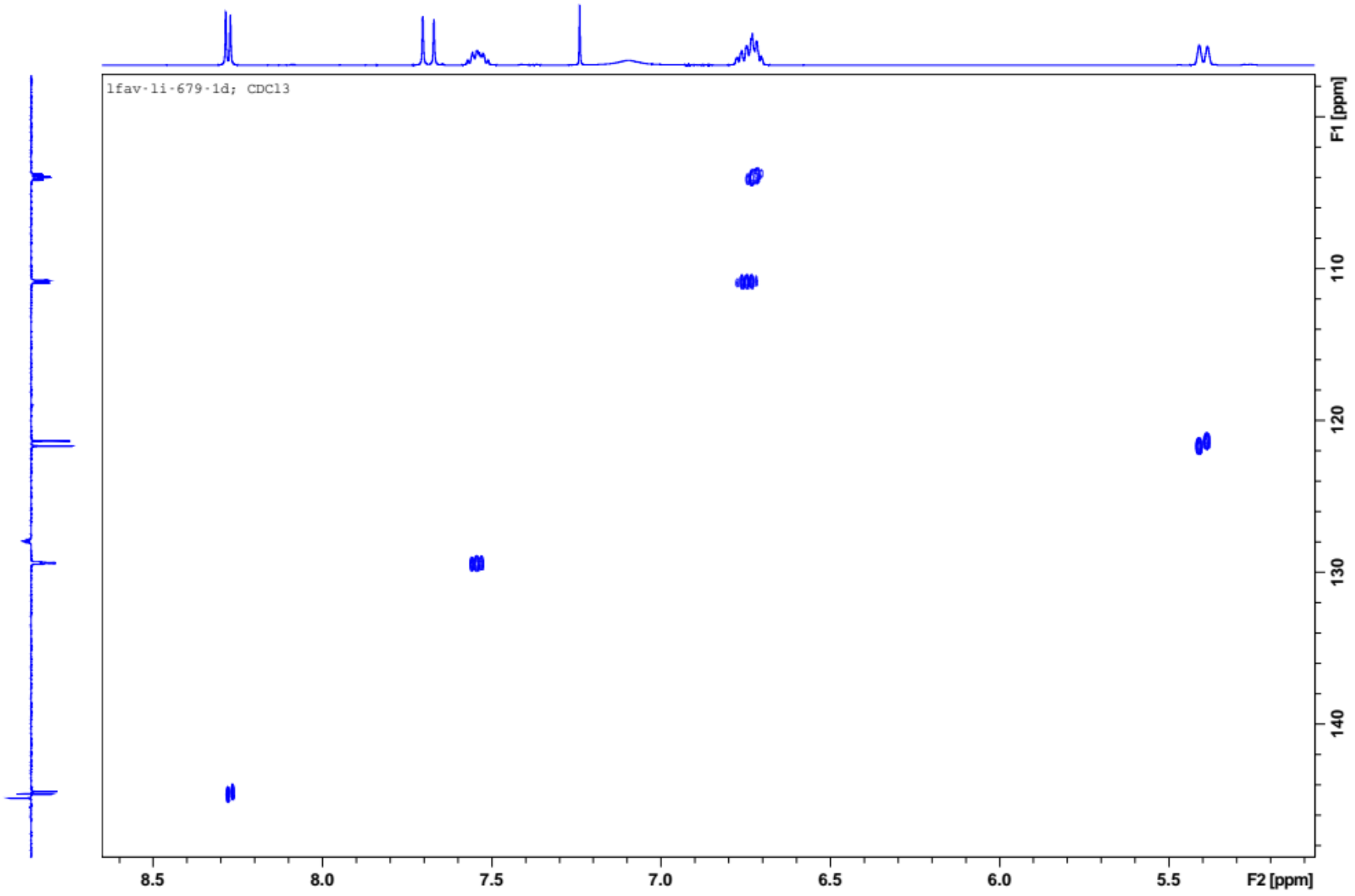

Figure S5 (continued).

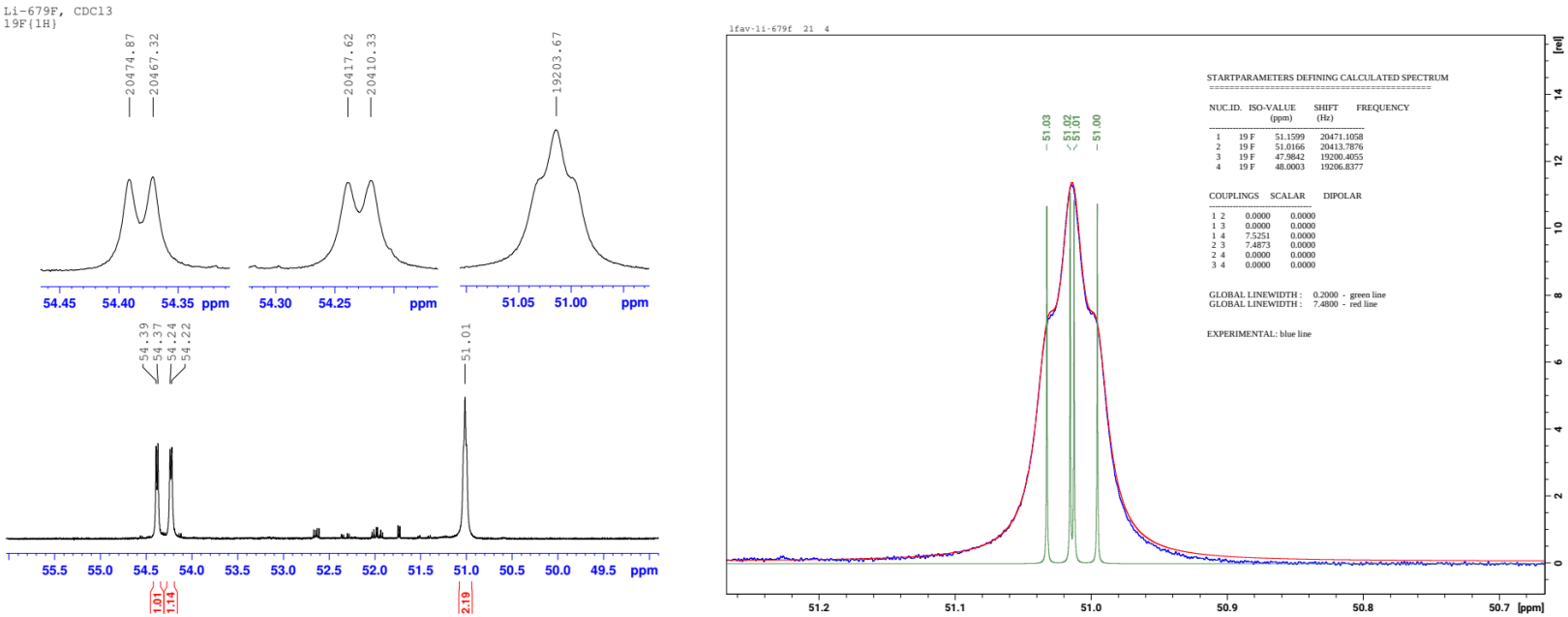

Figure S6 ^{19}F NMR spectrum of **2**.

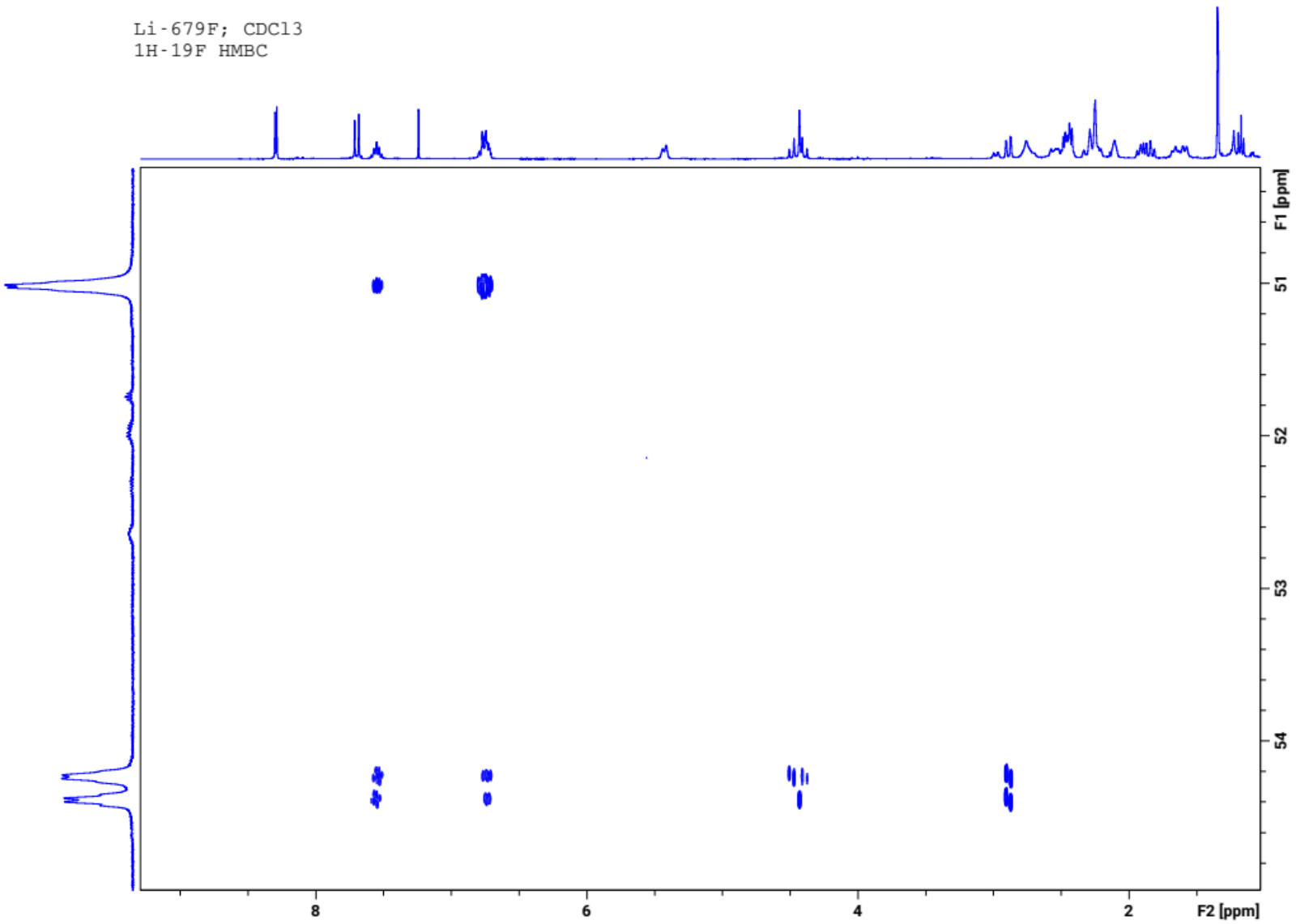

Figure S7 2D ^{1}H-^{19}F HMBC NMR spectrum of **2**.

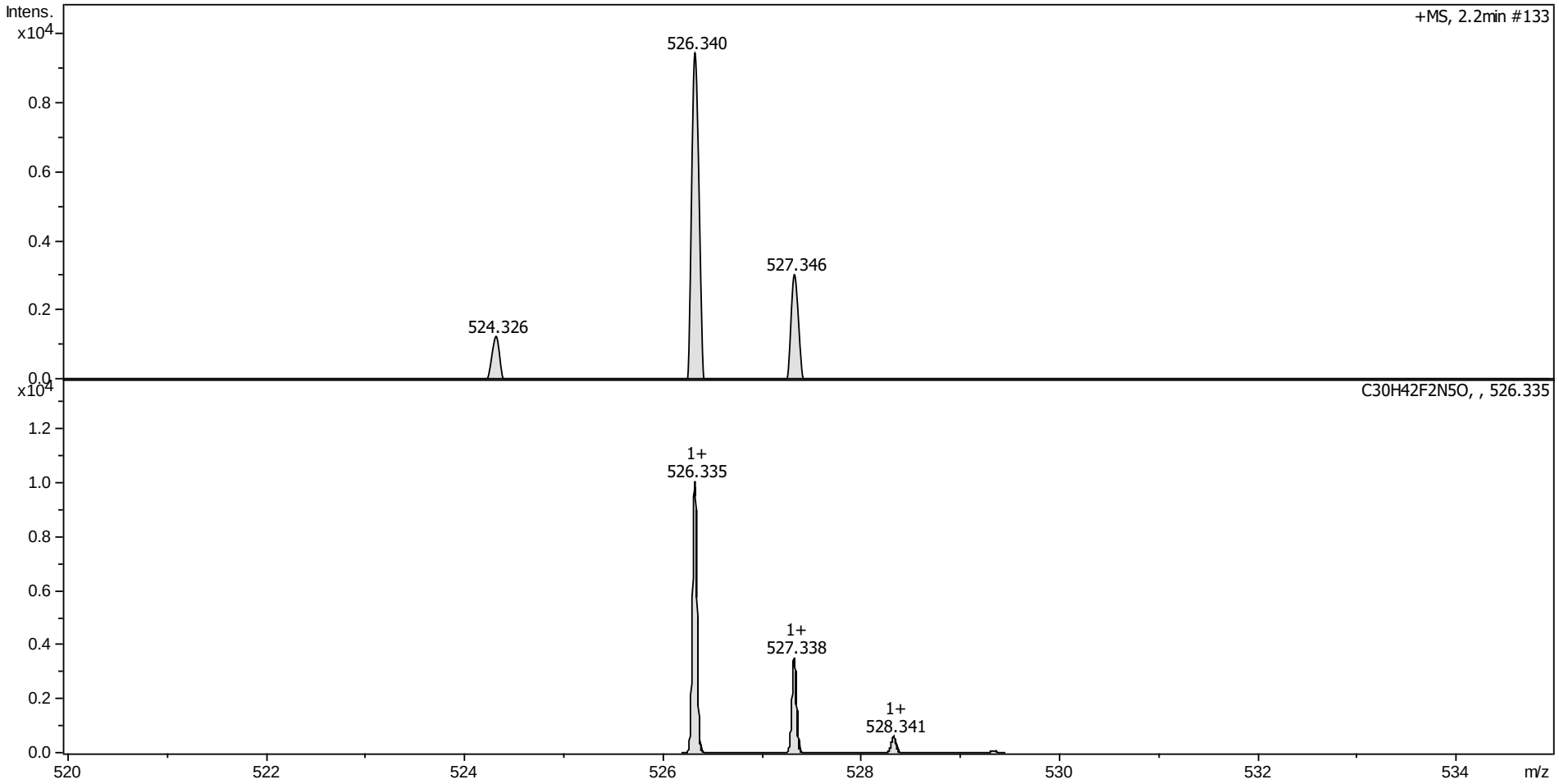

Figure S8 HRMS of the compound **10a** with simulation $C_{30}H_{42}N_5OF_2^+$.

Antifungal activity

Minimum inhibitory concentrations of the compounds were determined according to European Committee on Antimicrobial Susceptibility Testing (EUCAST) guidelines[S4]. Briefly, solutions of the compounds at desired concentrations were prepared in DMSO. Serial two-fold dilutions were obtained in cell culture-treated 96 well flat bottom microplates (Greiner Bio One International, Kremsmünster, Austria) using RPMI 1640 medium (SigmaAldrich, St. Louis, MO, USA) with L-glutamine, without sodium bicarbonate and 2% glucose, which were stored at −70 °C until used. For the test, the microplates were allowed to reach room temperature before inoculum (1–5 × 10^5 cfu/mL) was added, then they were incubated at 36 °C for 24 h. The absorbances of the wells were measured at 530 nm using a spectrophotometer (BioTek Instruments, Vinooski, VT, USA). MIC values were determined as ≥50% reduction in growth according to drug-free control. The activity of the compounds was tested at least twice against standard strains (*C. krusei* ATCC 6258, *C. parapsilosis* ATCC 22019, *C. parapsilosis* ATCC 90018, *C. glabrata* ATCC 90030, *C. albicans* ATCC 90028, *C. albicans* ATCC 64547, *C. tropicalis* ATCC 750) using fluconazole as positive control. The results are presented as ranges of MIC values from the repeated tests.

Molecular modeling

Enantiomers and ionization states of **2** were generated using Epik (2021-4, Schrödinger LLC, New York, NY, USA) and optimized LigPrep (2021-4, Schrödinger LLC, New York, NY, USA) and then optimized using MacroModel (2021-4, Schrödinger LLC, New York, NY, USA) according to the OPLS4 forcefield parameters (2021-4, Schrödinger LLC, New York, NY, USA)[S5]. Then, Gasteiger charges were added to the ligand atoms, and the ligands were converted to pdbqt using AutoDockTools (v1.5.7, The Scripps Research Institute, San Diego, CA, USA). CaCYP51 crystal structure (PDB ID: 5TZ1, resolution: 2.00 Å) was downloaded from the RCSB protein data bank (www.rcsb.org). Preparation of the protein and molecular docking with AutoDock (v4.2.6, The Scripps Research Institute, San Diego, CA, USA)[S6] was performed as described in our previous work.

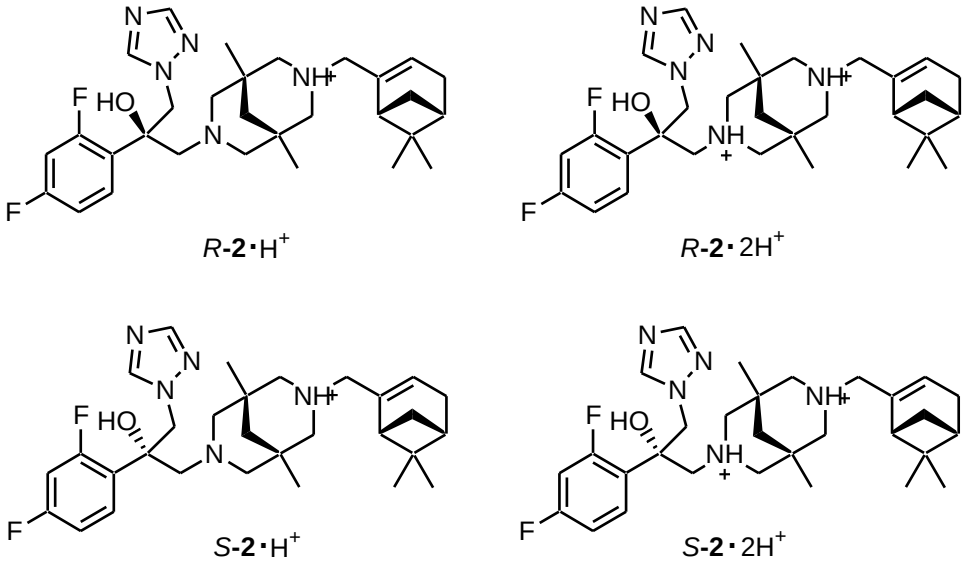

Figure S9 Enantiomers and ionization states of **2** predicted by molecular modeling.

Table S1. Docking scores of forms of compound **2**

Compound	Docking score (kcal mol^{-1})
R-**2**·H$^+$	-8.9
R-**2**·2H$^+$	-8.3
S-**2**·H$^+$	-7.4
Oteseconazole	-7.9

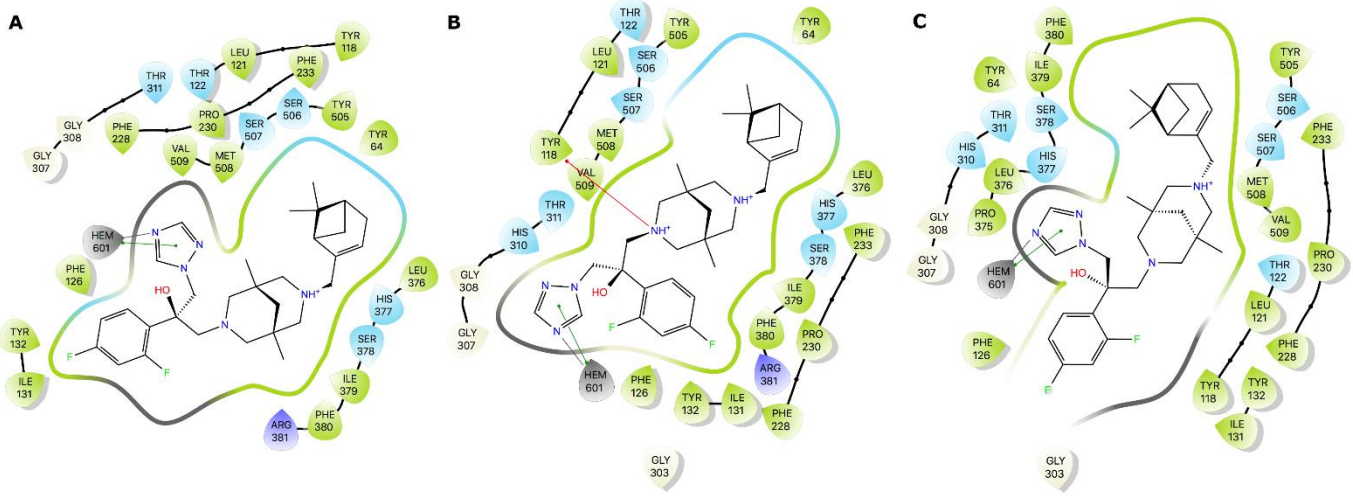

Figure S10 Predicted binding interactions of *R*-**2**·H$^+$, *R*-**2**·2H$^+$, *S*-**2**·H$^+$ and *S*-**2**·2H$^+$ in CaCYP51 active site represented as 2D diagrams.

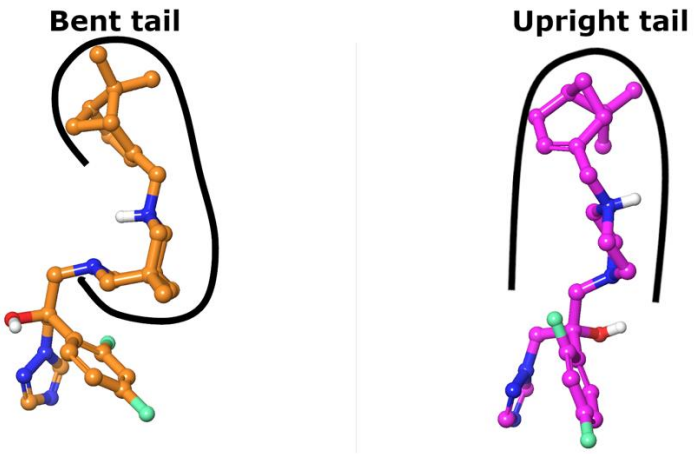

Figure S11 Binding conformations of *R*-**2**·H^+ (orange) and **1** (magenta)[S1] in CaCYP51 active site predicted by molecular docking.

Reference.

S1. N. S. Li-Zhulanov, N. P. Zaikova, S. Sari, D. Gülmez, S. Sabuncuoglu, K. Ozadali-Sari, S. Arikan-Akdagli, A. A. Nefedov, T. V. Rybalova, K. P. Volcho and N. F. Salakhutdinov, *Antibiotics*, 2023, **12**, 818.

S2. E. V. Suslov, K. Y. Ponomarev, O. S. Patrusheva, S. O. Kuranov, A. A. Okhina, A. D. Rogachev, A. A. Munkuev, R. V. Ottenbacher, A. I. Dalinger, M. A. Kalinin, S. Z. Vatsadze, K. P. Volcho and N. F. Salakhutdinov, *Molecules*, 2021, **26**, 7539.

S3. S. Z. Vatsadze, V. S. Tyurin, A. I. Zatsman, M. A. Manaenkova, V. S. Semashko, D. P. Krut'ko, N. V. Zyk, A. V. Churakov and L. G. Kuz'mina, *Russ. J. Org. Chem.*, 2006, **42**, 1225 (*Zh. Org. Khim*., 2006, **42**, 1244).

S4. M. C. M. J. Arendrup, J. W. Mouton, K. Lagrou, P. Hamal, J. Guinea and Subcommittee on Antifungal Susceptibility Testing (AFTS) of the ESCMID European Committee for Antimicrobial Susceptibility Testing (EUCAST), *EUCAST Antifungal MIC Method for Yeasts—Eucast Definitive Document E.DEF 7.3.2: Method for the Determination of Broth Dilution Minimum Inhibitory Concentrations of Antifungal Agents for Yeasts; EUCAST*: Copenhagen, Denmark, 2020. https://www.eucast.org/fileadmin/src/media/PDFs/EUCAST_files/AFST/Files/EUCAST_E_Def_7.3.2_Yeast_testing_definitive_revised_2020.pdf

S5. C. Lu, C. Wu, D. Ghoreishi, W. Chen, L. Wang, W. Damm, G. A. Ross, M. K. Dahlgren, E. Russell, C. D. von Bargen, R. Abel, R. A. Friesner and E. D. Harder, *J. Chem. Theory Comput*., 2021, **17**, 4291.

S6. G. M. Morris, R. Huey, W. Lindstrom, M. F. Sanner, R. K. Belew, D. S. Goodsell and A. J. Olson, *J. Comput. Chem*., 2009, **30**, 2785.